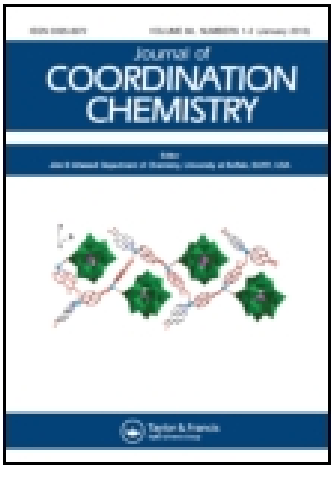

Journal of Coordination Chemistry
Publication details, including instructions for authors and subscription information:
http://www.tandfonline.com/loi/gcoo20

Facile synthesis, X-ray analysis, and spectroscopic studies of di-iron propanedithiolate complexes with tris(aromatic)phosphine ligands

Pei-Hua Zhao[a], Xin-Hang Li[a], Yun-Feng Liu[b] & Ya-Qing Liu[a]
[a] Research Center for Engineering Technology of Polymeric Composites of Shanxi Province, College of Materials Science and Engineering, North University of China, Taiyuan, PR China
[b] College of Public Health, Shanxi Medical University, Taiyuan, PR China

Accepted author version posted online: 12 Mar 2014.Published online: 04 Apr 2014.

To cite this article: Pei-Hua Zhao, Xin-Hang Li, Yun-Feng Liu & Ya-Qing Liu (2014) Facile synthesis, X-ray analysis, and spectroscopic studies of di-iron propanedithiolate complexes with tris(aromatic)phosphine ligands, Journal of Coordination Chemistry, 67:5, 766-778, DOI: 10.1080/00958972.2014.903329

To link to this article: http://dx.doi.org/10.1080/00958972.2014.903329

Journal of Coordination Chemistry, 2014
Vol. 67, No. 5, 766–778, http://dx.doi.org/10.1080/00958972.2014.903329

Facile synthesis, X-ray analysis, and spectroscopic studies of di-iron propanedithiolate complexes with tris(aromatic) phosphine ligands

PEI-HUA ZHAO*†, XIN-HANG LI†, YUN-FENG LIU‡ and YA-QING LIU*†

†Research Center for Engineering Technology of Polymeric Composites of Shanxi Province, College of Materials Science and Engineering, North University of China, Taiyuan, PR China
‡College of Public Health, Shanxi Medical University, Taiyuan, PR China

(*Received 8 January 2014; accepted 10 February 2014*)

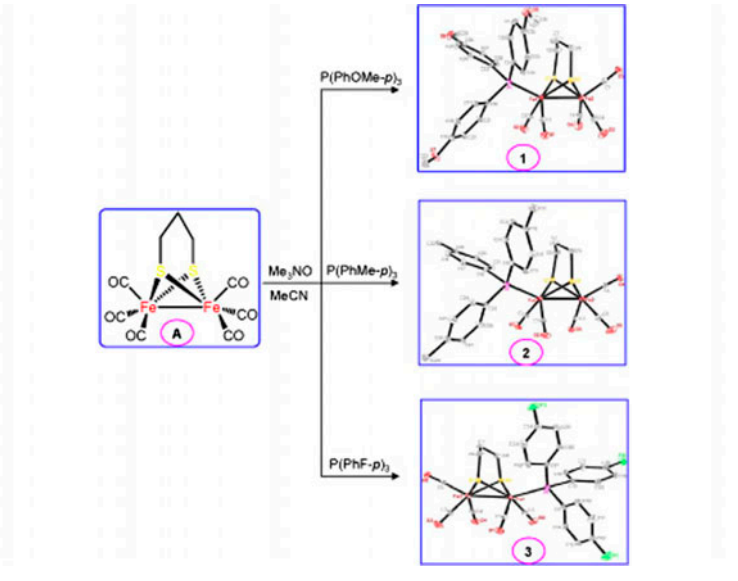

Three new propanedithiolate-type iron–sulfur complexes containing tris(aromatic)phosphine ligands, [{(μ-$SCH_2)_2CH_2$}$Fe_2(CO)_5$L] (L = P(PhOMe-*p*)$_3$, **1**; P(PhMe-*p*)$_3$, **2**; P(PhF-*p*)$_3$, **3**), have been prepared through carbonyl substitution in the presence of Me_3NO. The new complexes **1–3** were characterized by elemental analysis, IR, ^{1}H, ^{13}C{^{1}H}, and ^{31}P{H} NMR spectra. The molecular structures of **1–3** were unequivocally determined by single crystal X-ray diffraction, in which the tris(aromatic)phosphine coordinated to Fe resides in an apical position of the pseudo-square-pyramidal geometry. IR spectroscopy and X-ray crystallographic analysis for **1–3** have indicated that

*Corresponding authors. Email: zph2004@163.com (P.-H. Zhao); gczx2012@gmail.com (Y.-Q. Liu)

the highly electron rich tris(aromatic)phosphine ligands (where the corresponding electron-donating abilities display the following order of P(PhOMe-*p*)$_3$ > P(PhMe-*p*)$_3$ > P(PhF-*p*)$_3$) result in a considerable red shift of the CO-stretching frequencies and a clear change of the Fe–Fe bond distances in **1–3**.

Keywords: Iron–sulfur complexes; Tris(aromatic)phosphine; Carbonyl substitution; X-ray analysis; Spectroscopic study

1. Introduction

Chemistry of iron–sulfur complexes has attracted attention because of their close resemblance in structure to [FeFe]-hydrogenase, which is a type of nature's most efficient and inexpensive catalysts for hydrogen production [1–6]. High-resolution single-crystal X-ray crystallography has shown that [FeFe]-hydrogenase features a butterfly 2Fe2S subunit as its active site, where the iron centers are coordinated by carbonyl (CO)/cyanide (CN), a bridging dithiolate and a cysteinyl-S-linked cubic 4Fe4S cluster [7, 8].

The well-established structure of the aforementioned active site has provoked chemists to design and synthesize a number of iron–sulfur mimics of [FeFe]-hydrogenase. This can be achieved in two different strategies, one through substitution of CO groups to introduce electron-donating ligands, such as CN^- [9, 10], tertiary phosphine (PR_3) [11, 12], isonitrile [13, 14], and N-heterocyclic carbene [15, 16]; the other is by changing the bridgehead group or dichalcogenolate to modify the dithiolate linkers, including propanedithiolate (PDT) [17, 18], azadithiolate [19, 20], oxadithiolate [21, 22], thiodithiolate [23, 24], propanediselenoate [25, 26], azadiselenoate [27, 28], oxadiselenoate [29], thiodiselenoate [30], and propaneditelluroate [31] bridges. For the first approach, phosphine ligands are preferable in the [FeFe]-hydrogenase model system as a good substitute for naturally occurring CN^- [32]; for the second strategy, PDT-type iron–sulfur complexes have played an important role in the development of biomimetic chemistry of [FeFe]-hydrogenase [33–37].

On the basis of our previous study on PDT-type iron–sulfur complexes [38–40], we recently investigated the substitution reaction of [{(μ-SCH_2)$_2$$CH_2$}$Fe_2(CO)_6$] with interesting monophosphine ligands to further extend the iron–sulfur mimics of [FeFe]-hydrogenase, and have successfully prepared three new tris(aromatic)phosphine-substituted iron–sulfur complexes [{(μ-SCH_2)$_2$$CH_2$}$Fe_2(CO)_5$L] (L = P(PhOMe-*p*)$_3$, **1**; P(PhMe-*p*)$_3$, **2**; P(PhF-*p*)$_3$, **3**). Herein, we report the synthesis, spectroscopic characterization, and crystal structures of the PDT-type iron–sulfur complexes containing tris(aromatic)phosphine ligands.

2. Experimental

2.1. *Materials and methods*

All reactions and operations were carried out under a dry, oxygen-free nitrogen atmosphere with standard Schlenk and vacuum-line techniques. MeCN was distilled with CaH_2 under N_2. Commercially available materials, $Me_3NO{\cdot}2H_2O$, P(PhOMe-*p*)$_3$, P(PhMe-*p*)$_3$, and P(PhF-*p*)$_3$, were reagent grade and used as received. [{(μ-SCH_2)$_2$$CH_2$}$Fe_2(CO)_6$] (**A**) was prepared according to the literature [41]. Preparative TLC was carried out on glass plates (25 cm × 20 cm × 0.25 cm) coated with silica gel G (10–40 mm). IR spectra were recorded on a Nicolet 670 FTIR spectrometer. ^{1}H, ^{13}C{^{1}H}, and ^{31}P{H} NMR spectra were obtained

on a Bruker Avance 400 MHz spectrometer. Elemental analyses were performed on a Perkin-Elmer 240C analyzer. Melting points were determined on a YRT-3 apparatus and are uncorrected.

2.2. *Synthesis of [{(μ-SCH$_2$)$_2$CH$_2$}Fe$_2$(CO)$_5$P(PhOMe-p)$_3$] (1)*

A mixture of [{(μ-SCH$_2$)$_2$CH$_2$}Fe$_2$(CO)$_6$] (0.193 g, 0.5 mM), P(PhOMe-*p*)$_3$ (0.211 g, 0.6 mM), and Me$_3$NO·2H$_2$O (0.056 g, 0.5 mM) was dissolved in MeCN (15 mL) and was stirred at room temperature for 2 h to give a black-red solution. The solvent was removed on a rotary evaporator and the residue was subjected to preparative TLC separation using CH$_2$Cl$_2$/petroleum ether (v/v = 1 : 5) as eluent. From the main red band, **1** (0.241 g, 68%) was obtained as a red solid. M.p.: 180–181 °C. Anal. Calcd for C$_{29}$H$_{27}$Fe$_2$O$_8$PS$_2$: C, 49.04; H, 3.83%. Found: C, 48.93; H, 3.99%. IR (KBr disk, cm^{-1}): $\nu_{C\equiv O}$ 2041 (vs), 1985 (vs), 1979 (vs), 1958 (vs), 1930 (vs). ^{1}H NMR (400 MHz, CDCl$_3$, TMS, ppm): 7.58 (t, $^3J_{HH}$ = $^3J_{HP}$ = 7.6 Hz, 6H, Ph*H*), 6.93 (d, $^3J_{HH}$ = 7.6 Hz, 6H, Ph*H*), 3.84 (s, 9H, OC*H*$_3$), 1.78–1.72 (m, 2H, SCH$_a$*H*$_e$), 1.54–1.48 (m, 4H, SC*H*$_a$H$_e$ and C*H*$_2$). ^{13}C{^{1}H} NMR (100.6 MHz, CDCl$_3$, TMS, ppm): 213.92 (d, $^2J_{PC}$ = 12.0 Hz, PFe*C*O), 209.83 (s, Fe*C*O), 160.97 (s, *ipso*-Ph*C*OMe), 134.97 (d, $^2J_{PC}$ = 12.3 Hz, *o*-Ph*C*H), 127.55 (d, $^1J_{PC}$ = 44.8 Hz, *ipso*-Ph*C*P), 114.00 (d, $^3J_{PC}$ = 10.5 Hz, *m*-Ph*C*H), 55.37 (s, O*C*H$_3$), 30.02 (s, *C*H$_2$), 22.29 (s, S*C*H$_2$). ^{31}P{^{1}H} NMR (161.9 MHz, CDCl$_3$, 85% H$_3$PO$_4$, ppm): 60.26 (s).

2.3. *Synthesis of [{(μ-SCH$_2$)$_2$CH$_2$}Fe$_2$(CO)$_5$P(PhMe-p)$_3$] (2)*

The procedure was similar to that of **1** except P(PhMe-*p*)$_3$ (0.183 g, 0.6 mM) was used instead of P(PhOMe-*p*)$_3$ (0.211 g, 0.6 mM). Complex **2** (0.172 g, 52%) was obtained as a red solid. M.p.: 199–200 °C. Anal. Calcd for C$_{29}$H$_{27}$Fe$_2$O$_5$PS$_2$: C, 52.59; H, 4.11%. Found: C, 52.69; H, 4.03%. IR (KBr disk, cm^{-1}): $\nu_{C\equiv O}$ 2043 (vs), 1989 (vs), 1974 (vs), 1959 (vs), 1928 (vs). ^{1}H NMR (400 MHz, CDCl$_3$, TMS, ppm): 7.55 (t, $^3J_{HH}$ = $^3J_{HP}$ = 8.4 Hz, 6H, Ph*H*), 7.21 (d, $^3J_{HH}$ = 8.4 Hz, 6H, Ph*H*), 2.38 (s, 9H, PhC*H*$_3$), 1.75–1.69 (m, 2H, SCH$_a$*H*$_e$), 1.54–1.39 (m, 4H, SC*H*$_a$H$_e$ and C*H*$_2$). ^{13}C{^{1}H} NMR (100.6 MHz, CDCl$_3$, TMS, ppm): 213.82 (d, $^2J_{PC}$ = 10.7 Hz, PFe*C*O), 209.79 (s, Fe*C*O), 140.30 (s, *ipso*-Ph*C*Me), 133.48 (d, $^2J_{PC}$ = 11.4 Hz, *o*-Ph*C*H), 132.86 (d, $^1J_{PC}$ = 40.7 Hz, *ipso*-Ph*C*P), 129.24 (d, $^3J_{PC}$ = 9.7 Hz, *m*-Ph*C*H), 30.05 (s, *C*H$_2$), 22.21 (s, S*C*H$_2$), 21.44 (s, *C*H$_3$). ^{31}P{^{1}H} NMR (161.9 MHz, CDCl$_3$, 85% H$_3$PO$_4$, ppm): 62.38 (s).

2.4. *Synthesis of [{(μ-SCH$_2$)$_2$CH$_2$}Fe$_2$(CO)$_5$P(PhF-p)$_3$] (3)*

The procedure was similar to that of **1** except P(PhF-*p*)$_3$ (0.190 g, 0.6 mM) was used instead of P(PhOMe-*p*)$_3$ (0.211 g, 0.6 mM). Complex **3** (0.108 g, 32%) was obtained as a red solid. M.p.: 198–199 °C. Anal. Calcd for C$_{26}$H$_{18}$F$_3$Fe$_2$O$_5$PS$_2$: C, 46.32; H, 2.69%. Found: C, 46.20; H, 2.88%. IR (KBr disk, cm^{-1}): $\nu_{C\equiv O}$ 2048 (vs), 1979 (vs), 1972 (vs), 1954 (vs), 1932 (vs). ^{1}H NMR (400 MHz, CDCl$_3$, TMS, ppm): 7.63 (m, 6H, Ph*H*), 7.15 (t, $^3J_{HH}$ = $^3J_{HF}$ = 8.0 Hz, 6H, Ph*H*), 1.83–1.78 (m, 2H, SCH$_a$*H*$_e$), 1.54–1.48 (m, 4H, SC*H*$_a$H$_e$ and C*H*$_2$). ^{13}C{^{1}H} NMR (100.6 MHz, CDCl$_3$, TMS, ppm): 213.41 (d, $^2J_{PC}$ = 10.5 Hz, PFe*C*O), 209.24 (s, Fe*C*O), 164.00 (d, $^1J_{FC}$ = 253.2 Hz, *ipso*-Ph*C*F), 135.51 (dd, $^2J_{PC}$ = 12.5 Hz, $^3J_{FC}$ = 8.2 Hz, *o*-Ph*C*H), 131.41 (d, $^1J_{PC}$ = 40.8 Hz, *ipso*-Ph*C*P), 116.07

(d, $^3J_{PC}$ = 10.6 Hz, $^2J_{FC}$ = 21.1 Hz, *m*-Ph*C*H), 30.10 (s, *C*H_2), 22.37 (s, S*C*H_2). $^{31}P\{^1H\}$ NMR (161.9 MHz, $CDCl_3$, 85% H_3PO_4, ppm): 63.14 (s).

2.5. *X-ray structure determination*

Single crystals of **1–3** suitable for X-ray diffraction analysis were grown by slow evaporation of the CH_2Cl_2/hexane solution at 5 °C. Single crystals of **1–3** were mounted on a Rigaku MM-007 CCD diffractometer. Data were collected at 293(2) K for **1**, **2,** and **3** using a graphite monochromator with Mo Kα radiation (λ = 0.71073 Å) in the ω–φ scanning mode. Data collection, reduction, and absorption correction were performed by CRYSTALCLEAR [42]. The structure was solved by direct methods using SHELXS-97 [43] and refined by full-matrix least-squares (SHELXL-97) on F^2 [44]. Hydrogens were located using the geometric method.

3. Results and discussion

3.1. *Synthesis and spectroscopic studies*

The complexes **1–3** were readily prepared in moderate yields by reaction of [{(μ-SCH_2)$_2$$CH_2$}$Fe_2(CO)_6$] (**A**) with different tris(aromatic)phosphine ligands [namely, P(PhOMe-*p*)$_3$, P(PhMe-*p*)$_3$, or P(PhF-*p*)$_3$] using the decarbonylating agent Me_3NO in a 1 : 1.2 : 1 M ratio in MeCN at room temperature (scheme 1). The tris(aromatic)phosphine-

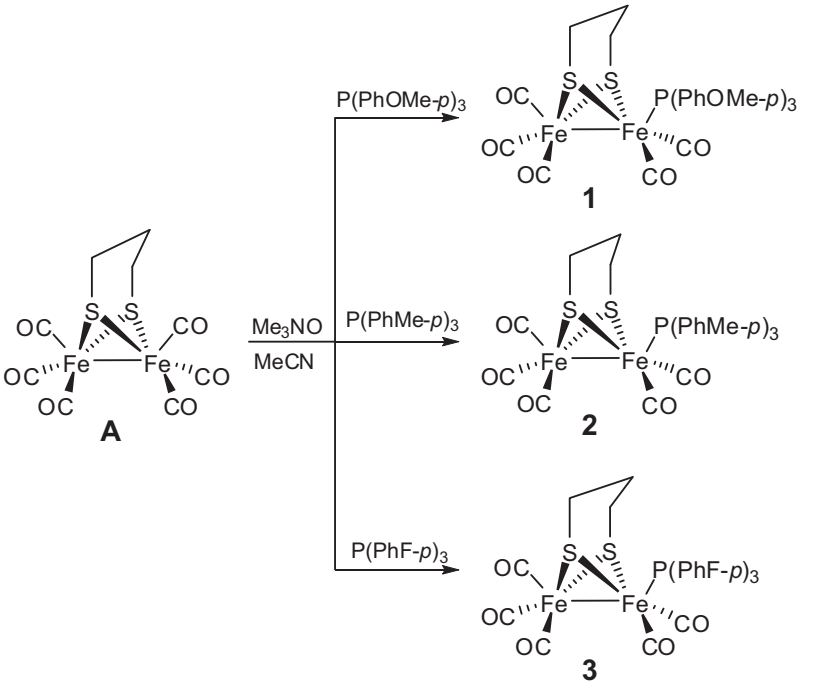

Scheme 1. Preparation of **1–3**.

monosubstituted products are soluble in polar organic solvents, such as CH_2Cl_2, EtOAc, THF, MeCN, etc. All the complexes are air stable in solution and in the solid state.

The complexes **1–3** are characterized by elemental analysis, IR, ^{1}H, ^{13}C{^{1}H}, and ^{31}P{H} NMR spectroscopy. The elemental analyses for **1–3** are in agreement with the respective compositions. The IR spectra of **1–3** in KBr exhibit three infrared absorptions from 2048–1928 cm^{-1} for terminally coordinated CO. IR data of ν(CO) bands are usually considered as a useful indicator for detecting variation in the electron density of Fe in di-iron CO complexes and evaluating the electron-donating abilities of the ligands coordinated to Fe. IR data of ν(CO) for **1–3** are compared to that of the parent complex (**A**) (table 1). The values of the highest ν(CO) bands for **1–3** are red shifted by 33, 31, and 27 cm^{-1} to lower frequencies as compared to that of the all-CO **A**, respectively, indicating that introduction of the highly electron rich tris(aromatic)phosphine ligands has a considerable enhancement of the electron density on the Fe cores. The order of red shifts of the highest ν(CO) bands for **1–3** indicate that the electron-donating abilities of three tris(aromatic)phosphine ligands exhibit the order, P(PhOMe-*p*)$_3$ > P(PhMe-*p*)$_3$ > P(PhF-*p*)$_3$, which can be attributed to the structural and electronic variations of the substituents of the aromatic rings in the corresponding phosphine ligands.

^{1}H NMR spectra of **1–3** display two multiplets at 1.83–1.69 and 1.54–1.39 ppm, which are assigned to resonances of the methylene protons in the PDT bridge. A sharp singlet at 3.84 ppm for the methoxy protons is observed in the ^{1}H NMR spectrum of **1**, while a strong singlet at 2.38 ppm for the methyl protons is present in the corresponding **2**. Furthermore, two types of peaks at 7.58 and 6.93 ppm for **1**, 7.55 and 7.21 ppm for **2**, as well as 7.63 and 7.15 ppm for **3** are ascribed to phenyl protons, indicating that OMe, Me, and F substituents in the tris(aromatic)phosphine ligands are located in the *para* position of the phenyls.

In the ^{31}C{^{1}H} NMR spectra, two peaks for bridging propane carbons are present at *ca.* 30/22 pm for **1–3**. The spectra of **1–3** display four peaks for phenyl carbons from 164 to 114 ppm, consistent with the different peaks for the phenyl protons in their ^{1}H NMR spectra. Furthermore, the spectra of **1–3** exhibit a doublet at 213 ppm with a $^2J_{PC}$ coupling constant (*ca.* 11 Hz) for the coordinated COs in the $PFe(CO)_2$ unit and a singlet at 209 ppm for the terminal COs of $Fe(CO)_3$ [40, 50]. In addition, the ^{31}P{^{1}H} NMR spectra of **1–3** show a sharp singlet at 60.26, 62.38, and 63.14 ppm for phosphorus of the coordinated tris(aromatic)phosphine ligands.

3.2. *X-ray crystallographic analysis*

The molecular structures of **1–3** have been further confirmed by X-ray crystallography (figures 1–3). The crystallographic parameters, data collection, and structure refinement of **1–3** are summarized in table 2. Selected bond lengths and angles are listed in table 3.

Table 1. A comparison of the ν(CO) bands for [{(μ-SCH$_2$)$_2$CH$_2$}Fe$_2$(CO)$_5$L] (L = CO, **A**; P(PhOMe-*p*)$_3$, **1**; P(PhMe-*p*)$_3$, **2**; P(PhF-*p*)$_3$, **3**).

Complex	L	ν(CO) (cm^{-1})	$\Delta\nu$(CO)$_{highest}$[a] (cm^{-1})	Note
1	P(PhOMe-*p*)$_3$	2041, 1985, 1979, 1958, 1930	−33	This work
2	P(PhMe-*p*)$_3$	2043, 1989, 1974, 1959, 1928	−31	This work
3	P(PhF-*p*)$_3$	2048, 1979, 1972, 1954, 1932	−26	This work
A	CO	2074, 2036, 1995	–	Ref. [47]

[a]$\Delta\nu = \nu(CO)_{substituted\text{-}CO} - \nu(CO)_{all\text{-}CO}$.

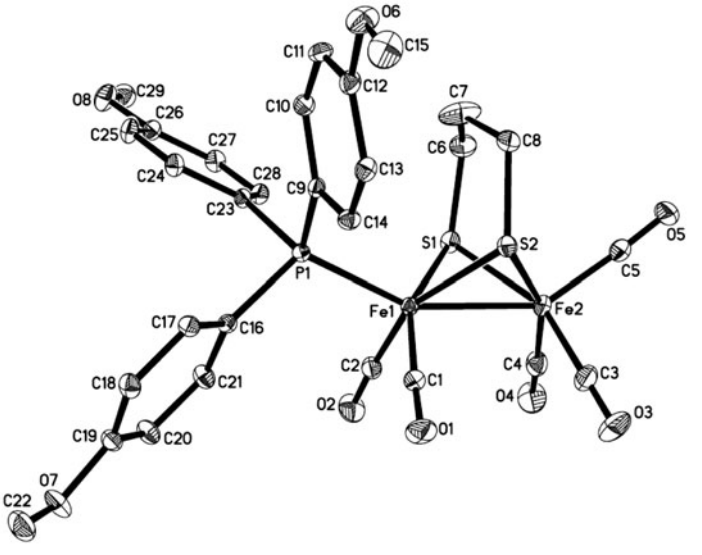

Figure 1. Molecular structure of **1** with thermal ellipsoid at 30% probability.

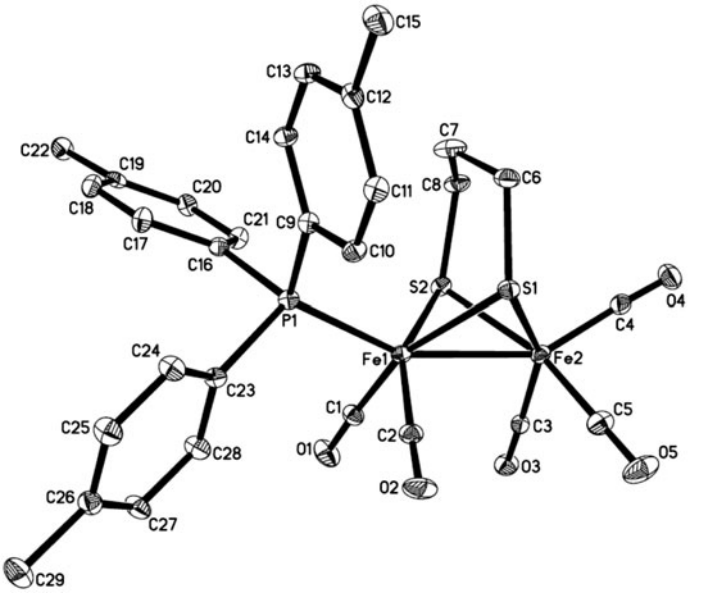

Figure 2. Molecular structure of **2** with thermal ellipsoid at 30% probability.

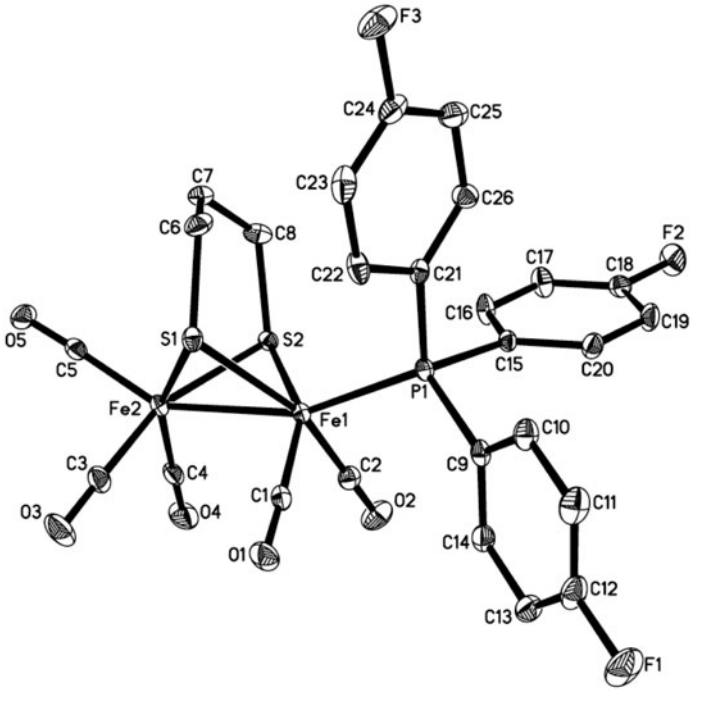

Figure 3. Molecular structure of **3** with thermal ellipsoid at 30% probability.

Single-crystal X-ray diffraction analysis reveals that the 2Fe2S skeleton of **1–3** has the expected butterfly conformation and each Fe displays distorted square-pyramidal coordination geometry, in accord with reported PDT-type iron–sulfur mimics of [FeFe]-hydrogenase [45–57]. Moreover, both $^{31}P\{H\}$-NMR and X-ray crystallographic analyses of **1–3** suggest that one CO-displacement by the tris(aromatic)phosphine ligands in the all-CO parent complex (**A**) affords only an apical isomer (figures 1–3). The corresponding ligands [i.e. P(PhOMe-*p*)$_3$, P(PhMe-*p*)$_3$ and P(PhF-*p*)$_3$] in **1–3** are coordinated to an apical site on one Fe and roughly *trans* to the Fe–Fe bond, consistent with those in the common configurations of the PR_3-monosubstituted complexes [$\{(\mu\text{-}SCH_2)_2CH_2\}Fe_2(CO)_5L$] (L = PPh_3 [45], $P(OEt)_3$ [45], $PhPMe_2$ [45], $PPh_2NH(2\text{-}NH_2Ph)$ [48], $PPh_2NH(CH_2)_2NMe_2$ [48], $PPh_2(2\text{-}NMe_2CH_2Ph)$ [48], $PPh_2(CH_2CO_2H)$ [49], $PPh_2(2\text{-}NHPy)$ [50], PPh_2Fc [51], and $PPh_2(H)C_{60}$ [52]) but different from basal and *cis* conformations of the previously reported analogs [$\{(\mu\text{-}SCH_2)_2CH_2\}Fe_2(CO)_5L$] (L = PTA [53], $P(NC_4H_8)_3$ [54], and $P(CH_2CH_2CO_2H)_3$ [55]).

The Fe–Fe distances in **1** (2.5166(7) Å), **2** (2.5144(10) Å), and **3** (2.5029(8) Å) are slightly longer or shorter than that of the parent [$\{(\mu\text{-}SCH_2)_2CH_2\}Fe_2(CO)_6$] (**A**) (2.5103(11) Å) [56], but these distances are shorter than that found in the natural [FeFe]-hydrogenase enzymes (2.55–2.60 Å) [7, 8]. It should be noted that substitution of CO with different tris(aromatic)phosphines which lie in an apical position of Fe(1) or Fe(2), enables Fe…Fe separations to be lengthened in **1** and **2**, but shortened in **3** as compared to that of the all-CO **A**. This may be because the electron-donating capabilities of the tris(aromatic)phosphines

Table 2. Crystal data and structural refinement details for **1–3**.

Complex	**1**	**2**	**3**
Empirical formula	$C_{29}H_{27}Fe_2O_8PS_2$	$C_{29}H_{27}Fe_2O_5PS_2$	$C_{26}H_{18}F_3Fe_2O_5PS_2$
Formula weight	710.29	662.30	674.19
Temperature (K)	293 (2)	293 (2)	293 (2)
Wavelength (Å)	0.71073	0.71073	0.71073
Crystal system	Triclinic	Monoclinic	Monoclinic
Space group	*P-1*	*P2(1)/n*	*P(2)1/n*
a (Å)	10.9434 (5)	14.1021 (10)	9.1082 (4)
b (Å)	11.5081 (6)	12.7469 (7)	8.5451 (5)
c (Å)	13.2598 (7)	16.9925 (12)	34.6865 (15)
α (°)	87.436 (4)	90	90
β (°)	86.194 (4)	106.983 (7)	91.864 (4)
γ (°)	67.398 (5)	90	90
V (Å^3)	1537.93 (14)	2921.3 (3)	2698.2 (2)
Z	2	4	4
D_{Calcd} (g cm^{-3})	1.532	1.506	1.660
μ (mm^{-1})	1.179	1.228	1.346
F (0 0 0)	726	1360	1360
Crystal size (mm)	0.30 × 0.20 × 0.20	0.30 × 0.22 × 0.18	0.26 × 0.20 × 0.03
θ_{min}, θ_{max} (°)	3.08, 26.37	2.97, 26.37	2.96, 26.37
Reflections collected/unique	11,241/6291	14,368/5924	12,359/5518
R_{int}	0.0343	0.0609	0.0386
hkl range	$-13 \le h \le 11$ $-13 \le k \le 14$ $-16 \le l \le 15$	$-16 \le h \le 17$ $-15 \le k \le 13$ $-17 \le l \le 21$	$-11 \le h \le 11$ $-9 \le k \le 10$ $-34 \le l \le 43$
Completeness to θ_{max} (%)	99.8	99.1	99.8
Data/restraints/parameters	6291/6/377	5924/0/355	5518/4/362
Goodness-of-fit (GOF) on F^2	1.033	1.024	1.109
R_1/wR_2 [$I > 2\sigma(I)$]	0.0508/0.0981	0.0621/0.0805	0.0537/0.0927
R_1/wR_2 (all data)	0.0807/0.1149	0.1225/0.1011	0.0805/0.1022
Largest difference peak/hole (e A^{-3})	0.937/−0.691	0.624/−0.394	0.416/−0.386

relative to the CO ligands display a resulting order of P(PhOMe-*p*)$_3$ > P(PhMe-*p*)$_3$ > P(PhF-*p*)$_3$ as observed in IR spectra of **1–3**. Meanwhile, the average Fe–S distances [**1**: (2.2590 Å); **2**: (2.2618 Å); **3**: (2.2675 Å)] and the Fe–P distances [**1**: (2.2482(11) Å); **2**: (2.2372(14) Å); **3**: (2.2425(11) Å)] are comparable to each other and to the corresponding lengths reported for PR_3-coordinated iron–sulfur analogs [51, 52]. In the case of **1–3**, the average Fe–C_{CO} distances of the coordinated-Fe center [**1**: (1.760 Å); **2**: (1.762 Å); **3**: (1.763 Å)] are notably shorter than the corresponding lengths of the uncoordinated-Fe [**1**: (1.789 Å); **2**: (1.786 Å); **3**: (1.785 Å)]. Accordingly, the average C–O distances in the $Fe(CO)_2L$ unit [**1**: (1.142 Å); **2**: (1.148 Å); **3**: (1.141 Å)] are a bit longer than the corresponding lengths in the $Fe(CO)_3$ unit [**1**: (1.137 Å); **2**: (1.141 Å); **3**: (1.137 Å)]. A reasonable explanation is that the higher electron density of the coordinated-Fe leads to stronger electron back-donation from the coordinated-Fe to CO in $Fe(CO)_2L$ relative to the back-donation from the uncoordinated-Fe to CO in $Fe(CO)_3$ [26, 57].

The dihedral angles, defined by S(1)–Fe(1)–Fe(2) and S(2)–Fe(1)–Fe(2) planes, are 108.1, 72.1, and 107.1 in **1–3**, respectively, and different from each other, implying that self-regulation of the central 2Fe2S skeleton is accompanied by variation of the electron-densities on the Fe core for molecular stability. The angles of P(1)–Fe(1)–Fe(2) are 8.47, 4.75, and 7.56, larger than the ones of C(5)–Fe(2)–Fe(1), C(4)–Fe(2)–Fe(1), and C(5)–Fe(2)–Fe(1) in **1–3**, respectively, demonstrating that steric effects of the tris(aromatic)

Table 3. Selected bond lengths (Å) and angles (°) for **1–3**.

Complex	**1**	**2**	**3**
Fe(1)–Fe(2)	2.5166 (7)	2.5144 (10)	2.5029 (8)
Fe(1)–S(2)	2.2590 (11)	2.2757 (13)	2.2780 (11)
Fe(1)–S(1)	2.2630 (11)	2.2579 (14)	2.2652 (12)
Fe(2)–S(1)	2.2564 (12)	2.2574 (13)	2.2661 (11)
Fe(2)–S(2)	2.2576 (12)	2.2563 (14)	2.2606 (10)
O(1)–C(1)	1.139 (5)	1.147 (5)	1.145 (4)
O(2)–C(2)	1.145 (5)	1.149 (5)	1.137 (5)
O(3)–C(3)	1.137 (5)	1.136 (5)	1.138 (5)
S(2)–Fe(1)–S(1)	84.41 (4)	84.24 (5)	84.09 (4)
S(2)–Fe(1)–Fe(2)	56.11 (3)	55.94 (4)	56.20 (3)
S(1)–Fe(1)–Fe(2)	56.04 (3)	56.15 (4)	56.49 (3)
Fe(2)–S(1)–Fe(1)	67.67 (3)	67.68 (4)	67.06 (3)
C(2)–Fe(1)–Fe(2)	100.39 (13)	98.72 (18)	101.49 (13)
C(1)–Fe(1)–Fe(2)	99.72 (13)	102.30 (17)	96.66 (13)
P(1)–Fe(1)–Fe(2)	154.80 (4)	155.64 (5)	158.83 (4)
C(6)–S(1)–Fe(2)	110.04 (17)	112.79 (17)	111.21 (14)
C(6)–S(1)–Fe(1)	115.22 (17)	114.05 (18)	114.80 (16)
Fe(1)–P(1)	2.2482 (11)	2.2372 (14)	2.2425 (11)
Fe(1)–C(2)	1.757 (4)	1.757 (5)	1.762 (4)
Fe(1)–C(1)	1.763 (4)	1.767 (5)	1.763 (5)
Fe(2)–C(4)	1.786 (6)	1.776 (6)	1.797 (5)
Fe(2)–C(3)	1.788 (5)	1.787 (5)	1.780 (4)
Fe(2)–C(5)	1.794 (5)	1.794 (6)	1.779 (5)
O(4)–C(4)	1.138 (6)	1.137 (5)	1.141 (5)
O(5)–C(5)	1.137 (5)	1.150 (5)	1.133 (5)
S(1)–Fe(2)–S(2)	84.60 (4)	84.70 (5)	84.47 (4)
S(1)–Fe(2)–Fe(1)	56.29 (3)	56.17 (4)	56.45 (3)
S(2)–Fe(2)–Fe(1)	56.16 (3)	56.67 (4)	56.87 (3)
Fe(2)–S(2)–Fe(1)	67.72 (3)	67.39 (4)	66.94 (3)
C(4)–Fe(2)–Fe(1)	103.31 (14)	150.89 (16)	99.81 (15)
C(3)–Fe(2)–Fe(1)	100.82 (15)	95.66 (16)	102.45 (14)
C(5)–Fe(2)–Fe(1)	146.33 (14)	106.3 (2)	151.27 (13)
C(8)–S(2)–Fe(2)	111.70 (16)	109.69 (18)	110.75 (16)
C(8)–S(2)–Fe(1)	114.93 (15)	115.54 (17)	116.79 (15)

phosphine ligands on the structures of **1–3** exhibit the following order: P(PhOMe-*p*)$_3$ > P(PhF-*p*)$_3$ > P(PhMe-*p*)$_3$. The differences between [C(6)–S(1)–Fe(1) *versus* C(6)–S(1)–Fe(2)/C(8)–S(2)–Fe(1) *versus* C(8)–S(2)–Fe(2) in **1–3**] are 5.18/3.23, 1.26/5.85, and 3.59/6.04, respectively. This indicates that the FeS_2C_3 six-member ring of 1,3-PDT in **1–3** is pushed away from the site occupied by an apical P(PhOMe-*p*)$_3$, P(PhMe-*p*)$_3$, or P(PhF-*p*)$_3$ owing to the steric effect [46], which results in tilt of the iron-dithiacyclohexane ring towards the Fe(CO)$_3$ site.

It can be concluded from the above X-ray crystallographic discussions that coordination geometry of the PDT-type iron–sulfur complexes is mainly determined by electron-donating abilities and steric effects of the coordinated ligands, which are bound to the Fe core in the butterfly 2Fe2S structure.

Solid-state structures of **1–3** were stabilized by van der Waals' interactions and π–π stacking observed in their crystal packing diagrams (figures 4–6).

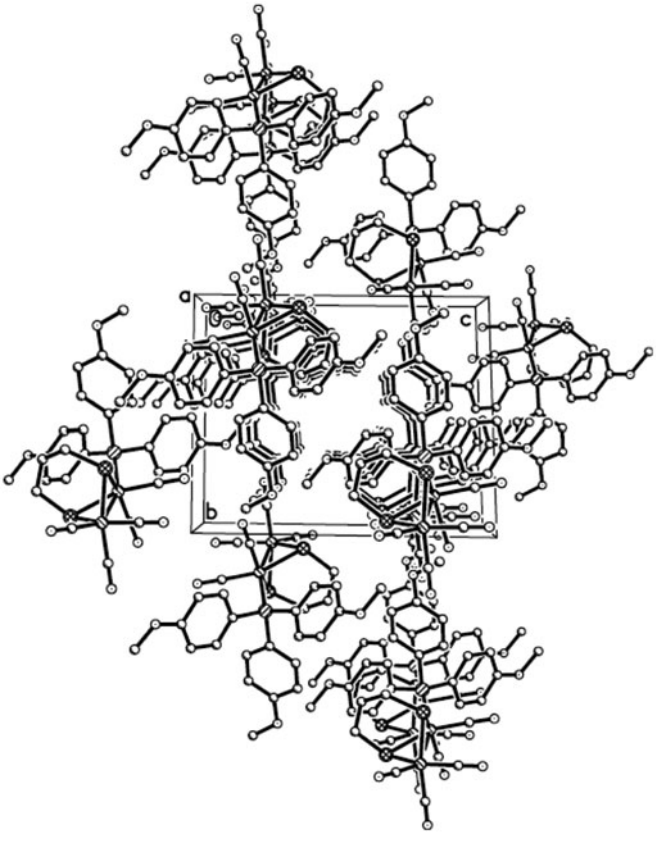

Figure 4. Crystal packing diagram of **1** along the *a*-axis.

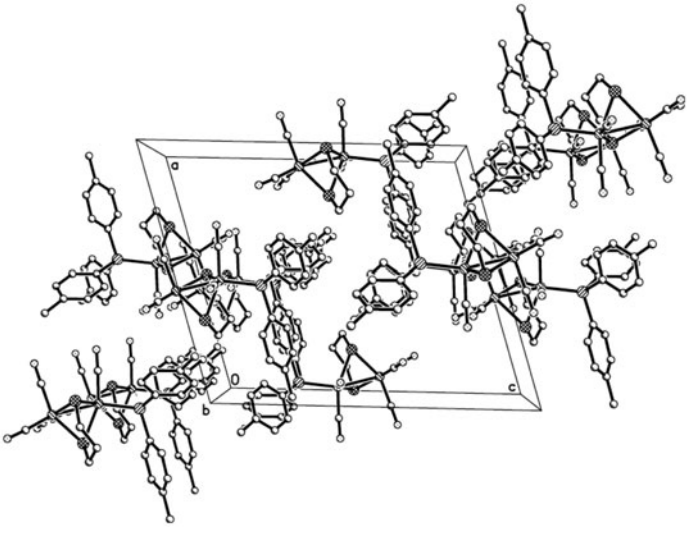

Figure 5. Crystal packing diagram of **2** along the *b*-axis.

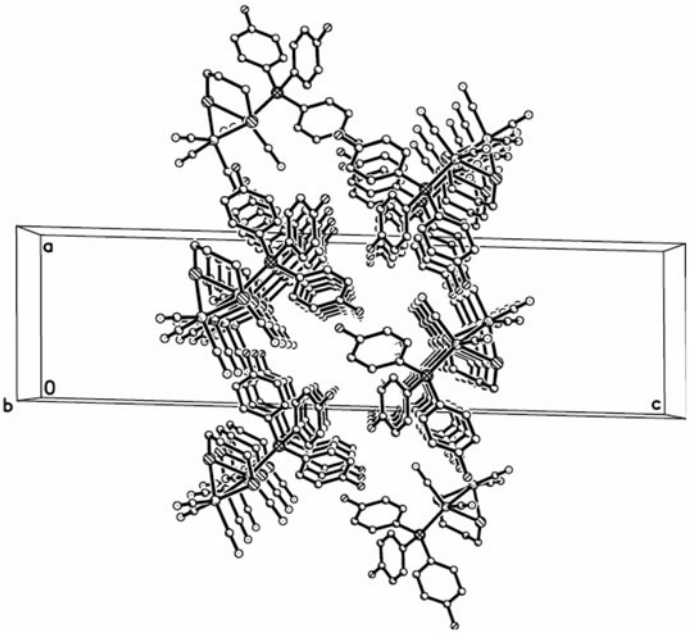

Figure 6. Crystal packing diagram of **3** along the *b*-axis.

4. Conclusion

We have synthesized four new tris(aromatic)phosphine-substituted PDT-type iron–sulfur complexes, **1–3**, which are regarded as iron–sulfur mimics of [FeFe]-hydrogenase. All the complexes are fully characterized by IR and NMR spectroscopic analyses and also by single-crystal X-ray structures. IR spectroscopic and X-ray crystallographic studies indicated electron-donating abilities of the tris(aromatic)phosphine ligands in the order $P(PhOMe\text{-}p)_3 > P(PhMe\text{-}p)_3 > P(PhF\text{-}p)_3$ lead to increased electron density at the iron centers and further cause considerable red shift of the CO-stretching frequencies, and change in the Fe–Fe bond distances in **1–3**.

Supplementary material

CCDC-952267 (**1**), CCDC-952266 (**2**), and CCDC-952264 (**3**) contain the supplementary crystallographic data for this paper. These data can be obtained free of charge via http://www.ccdc.cam.ac.uk/conts/retrieving.html, or from the Cambridge Crystallographic Data Center, 12 Union Road Cambridge CB2 1EZ, UK; Fax: (+44) 1223-336-033; or E-mail: deposit@ccdc.cam.ac.uk.

Funding

This work was financially supported by the National Natural Science Foundation of China [grant number 21301160] and the Natural Science Foundation for Young Scholars of Shanxi Province [grant number 2012021007-4].

References

[1] J.-F. Capon, F. Gloaguen, P. Schollhammer, J. Talarmin. *Coord. Chem. Rev.*, **249**, 1664 (2005).
[2] L.-C. Song. *Acc. Chem. Res.*, **38**, 21 (2005).
[3] C. Tard, C.J. Pickett. *Chem. Rev.*, **109**, 2245 (2009).
[4] F. Wang, W.-G. Wang, H.-Y. Wang, G. Si, C.-H. Tung, L.-Z. Wu. *ACS Catal.*, **2**, 407 (2012).
[5] X.-F. Liu, X.-W. Xiao, L.-J. Shen. *J. Coord. Chem.*, **64**, 1023 (2011).
[6] M. Karnahl, A. Orthaber, S. Tschierlei, L. Nagarajan, S. Ott. *J. Coord. Chem.*, **65**, 2713 (2012).
[7] J.W. Peters, W.N. Lanzilotta, B.J. Lemon, L.C. Seefeldt. *Science*, **282**, 1853 (1998).
[8] Y. Nicolet, C. Piras, P. Legrand, C.E Hatchikian, J.C. Fontecilla-Camps. *Structure*, **7**, 13 (1999).
[9] A. Le Cloirec, S.C. Davies, D.J. Evans, D.L. Hughes, C.J. Pickett, S.P. Best, S. Borg. *Chem. Commun.*, **22**, 2285 (1999).
[10] F. Gloaguen, J.D. Lawrence, M. Schmidt, S.R. Wilson, T.B. Rauchfuss. *J. Am. Chem. Soc.*, **123**, 12518 (2001).
[11] (a) T.-H. Yen, K.-T. Chu, W.-W. Chiu, Y.-C. Chien, G.-H. Lee, M.-H. Chiang. *Polyhedron*, **64**, 247 (2013); (b) X.-F. Liu, H.-Q. Gao. *Polyhedron*, **65**, 1 (2013).
[12] (a)X.-F. Liu. *Inorg. Chim. Acta*, **378**, 338 (2011); (b) X.-F. Liu, M.-Y. Chen, H.-Q. Gao. *J. Coord. Chem.*, **67,** 57 (2014).
[13] (a) J.L. Nehring, D.M. Heinekey. *Inorg. Chem.*, **42**, 4288 (2003); (b) X.-F. Liu. *J. Organomet. Chem.*, **750**, 117 (2014).
[14] J. Hou, X.-J. Peng, J.-F. Liu, Y.-L. Gao, X. Zhao, S. Gao, K.-L. Han. *Eur. J. Inorg. Chem.*, **2006**, 4679 (2006).
[15] J.-F. Capon, S. El Hassnaoui, F. Gloaguen, P. Schollhammer, J. Talarmin. *Organometallics*, **24**, 2020 (2005).
[16] L.-C. Song, X. Luo, Y.-Z. Wang, B. Gai, Q.-M. Hu. *J. Organomet. Chem.*, **694**, 103 (2009).
[17] S. Salyi, M. Kritikos, B. Åkermark, L. Sun. *Chem. Eur. J.*, **9**, 557 (2003).
[18] U.-P. Apfel, C.R. Kowol, F. Kloss, H. Görls, B.K. Keppler, W. Weigand. *J. Organomet. Chem.*, **696**, 1084 (2011).
[19] J.D. Lawrence, H. Li, T.B. Rauchfuss, M. Bénard, M.M. Rohmer. *Angew. Chem. Int. Ed.*, **40**, 1768 (2001).
[20] P.-H. Zhao, Y.-Q. Liu, X.-H. Li. *Asian J. Chem.*, **25**, 5428 (2013).
[21] L.-C. Song, Z.-Y. Yang, H.-Z. Bian, Q.-M. Hu. *Organometallics*, **23**, 3082 (2004).
[22] L.-C. Song, Z.-Y. Yang, H.-Z. Bian, Y. Liu, H.-T. Wang, X.-F. Liu, Q.-M. Hu. *Organometallics*, **24**, 6126 (2005).
[23] J. Windhager, M. Rudolph, S. Bräutigam, H. Görls, W. Weigand. *Eur. J. Inorg. Chem.*, **2007,** 2748 (2007).
[24] L.-C. Song, Z.-Y. Yang, Y.-J. Hua, H.-T. Wang, Y. Liu, Q.-M. Hu. *Organometallics*, **26**, 2106 (2007).
[25] L.-C. Song, B. Gai, H.-T. Wang, Q.-M. Hu. *J. Inorg. Biochem.*, **103**, 805 (2009).
[26] M. El-khateeb, M. Harb, Q. Abu-Salem, H. Görls, W. Weigand. *Polyhedron*, **61**, 1 (2013).
[27] S. Gao, J.-L. Fan, S.-G. Sun, X.-J. Peng, X. Zhao, J. Hou. *Dalton Trans.*, 2128 (2008).
[28] Y.-L. Li, B. Xie, L.-K. Zou, X.-L. Zhang, X. Lin. *J. Organomet. Chem.*, **718**, 74 (2012).
[29] L.-C. Song, B. Gai, Z.-H. Feng, Z.-Q. Du, Z.-J. Xie, X.-J. Sun, H.-B. Song. *Organometallics*, **32**, 3673 (2013).
[30] M.K. Harb, J. Windhager, T. Niksch, H. Görls, T. Sakamoto, E.R. Smith, R.S. Glass, D.L. Lichtenberger, D.H. Evans, M. El-khateeb, W. Weigand. *Tetrahedron*, **68**, 10592 (2012).
[31] L.-C. Song, Q.-L. Li, Z.-H. Feng, X.-J. Sun, Z.-J. Xie, H.-B. Song. *Dalton Trans.*, 1612 (2013).
[32] Y. Nicolet, B.J. Lemon, J.C. Fontecilla-Camps, J.W. Peters. *Trends Biochem. Sci.*, **25**, 138 (2000).
[33] D. Seyferth, R.S. Henderson, L.-C. Song. *J. Organomet. Chem.*, **192**, C1 (1980).
[34] H.G. Cui, M. Wang, L.L. Duan, L. Sun. *J. Coord. Chem.*, **61**, 1856 (2008).
[35] X.-F. Liu, B.-S. Yin. *J. Coord. Chem.*, **63**, 4061 (2010).
[36] C.A. Mebi, D.S. Karr, R.X. Gao. *J. Coord. Chem.*, **64**, 4397 (2011).
[37] (a) B.-S. Yin, T.-B. Li, M.-S. Yang. *J. Coord. Chem.*, **64**, 2066 (2011); (b) S. Ghosh, G. Hogarth, N. Hollingsworth, K.B. Holt, S.E. Kabir, B.E. Sanchez. *Chem. Commun.*, **50**, 945 (2014).
[38] L.-C. Song, P.-H. Zhao, Z.-Q. Du, M.-Y. Tang, Q.-M. Hu. *Organometallics*, **29**, 5751 (2010).
[39] L.-C. Song, X.-J. Sun, P.-H. Zhao, J.-P. Li, H.-B. Song. *Dalton Trans.*, 8941 (2012).
[40] P.-H. Zhao, Y.-Q. Liu, G.-Z. Zhao. *Polyhedron*, **53**, 144 (2013).
[41] E.J. Lyon, I.P. Georgakaki, J.H. Reibenspies, M.Y. Darensbourg. *Angew. Chem. Int. Ed.*, **38**, 3178 (1999).
[42] *CRYSTALCLEAR 1.3.6*. Rigaku and Rigaku/MSC, The Woodlands, TX (2005).
[43] G.M. Sheldrick. *SHELXS97, A Program for Crystal Structure Solution*, University of Göttingen, Germany (1997).
[44] G.M. Sheldrick. *SHELXL97, A Program for Crystal Structure Refinement*, University of Göttingen, Germany (1997).
[45] P. Li, M. Wang, C. He, G. Li, X. Liu, C. Chen, B. Åkermark, L. Sun. *Eur. J. Inorg. Chem.*, **2005**, 2506 (2005).
[46] S. Gao, H.-L. Guo, X.-J. Peng, X. Zhao, Q. Duan, Q.-C. Liang, D.-Y. Jiang. *New J. Chem.*, **37**, 1437 (2013).

[47] D. Chong, I.P. Georgakaki, R. Mejia-Rodriguez, J. Sanabria-Chinchilla, M.P. Soriaga, M.Y. Darensbourg. *Dalton Trans.*, 4158 (2003).
[48] Z. Wang, W.-F. Jiang, J.-H. Liu, W.-N. Jiang, Y. Wang, B. Åkermark, L. Sun. *J. Organomet. Chem.*, **693**, 2828 (2008).
[49] Z.-B. Zhao, M. Wang, W.-B. Dong, P. Li, Z. Yu, L. Sun. *J. Organomet. Chem.*, **694**, 2309 (2009).
[50] X.-F. Liu, X.-W. Xiao. *J. Organomet. Chem.*, **696**, 2767 (2011).
[51] Y.-C. Liu, C.-H. Lee, G.-H. Lee, M.-H. Chiang. *Eur. J. Inorg. Chem.*, **2011**, 1155 (2011).
[52] Y.-C. Liu, T.-H. Yen, Y.-J. Tseng, C.-H. Hu, G.-H. Lee, M.-H. Chiang. *Inorg. Chem.*, **51**, 5997 (2012).
[53] R. Mejia-Rodriguez, D. Chong, J.H. Reibenspies, M.P. Soriaga, M.Y. Darensbourg. *J. Am. Chem. Soc.*, **126**, 12004 (2004).
[54] J. Hou, X.-J. Peng, Z.-Y. Zhou, S.-G. Sun, X. Zhao, S. Gao. *J. Organomet. Chem.*, **691**, 4633 (2006).
[55] C.M. Thomas, O. Rüdiger, T.B. Liu, C.E. Carson, M.B. Hall, M.Y. Darensbourg. *Organometallics*, **26**, 3976 (2007).
[56] E.J. Lyon, I.P. Georgakaki, J.H. Reibenspies, M.Y. Darensbourg. *Angew. Chem. Int. Ed.*, **38**, 3178 (1999).
[57] G. Durgaprasad, R. Bolligarla, S.K. Das. *J. Organomet. Chem.*, **696**, 3097 (2011).